Materials Science Forum Vols 519-521 (2006) pp 621-628 *Online: 2006-07-15*

doi:10.4028/www.scientific.net/MSF.519-521.621

Surface Science Studies of the Effect of Al Alloy Microstructure on the Formation of Chromate Coatings

S.A. Kulinich, A.S. Akhtar, D. Susac, K.C. Wong, P.C. Wong and K.A.R. Mitchell[a]

Department of Chemistry, University of British Columbia,
2036 Main Mall, Vancouver, BC, Canada V6T 1Z1

[a] karm@chem.ubc.ca

Keywords: Aluminum alloy; Chromate conversion coating; Photoelectron spectroscopy; Scanning electron microscopy; Scanning Auger microscopy; Raman spectroscopy

Abstract. Surface science methods including scanning Auger microscopy (SAM), scanning electron microscopy (SEM), X-ray photoelectron spectroscopy (XPS) and Raman spectroscopy have been used to study the initial growth of chromate conversion coatings on aluminum 2024-T3 alloy, using a coating bath formed by dissolving CrO_3, $Na_2Cr_2O_7$ and NaF in water. The objective is to learn more about growth mechanism on the different microstructural regions of this alloy surface, including the second-phase particles and the alloy matrix.

Introduction

Industrial applications of aluminum and other light metal alloys depend on the ability to protect against corrosion with environmentally-friendly coatings [1-5]. In general, it is believed that the integrity of a coated material in a reactive environment depends on the nature and structure of the coating, as well as on the microstructure of the alloy itself [5-9]. The existence of such mechanistic knowledge should help the design of new coating procedures. This is especially important for the replacement of the chromate conversion coatings (CCCs) that have been traditionally used for the anticorrosive protection of aluminum alloys, given the legislative limitations on their continued use. While the microstructure of the alloy AA-2024-T3, widely used in aerospace applications, has been the subject of extensive investigation [10,11], studies of the mechanisms of CCC growth on this alloy remain quite limited [6,7,9,12], and the present work continues study in this area.

This program used AA-2024-T3 plates (1x1 cm^2) which had been mirror polished and degreased prior to dipping in a room-temperature CCC bath (formed from 4 g CrO_3, 3.5 g $Na_2Cr_2O_7$ and 0.8 g NaF per L of water as used previously [6,13]) for periods between 3 s and 2 min. Measurements with scanning Auger microscopy (SAM), X-ray photoelectron spectroscopy (XPS) and scanning electron microscopy (SEM) followed methods described elsewhere in this volume [14]. Raman spectra were acquired with a Renishaw inVia microscope using a He-Ne laser (632.8 nm) following standard procedures.

Results and discussion

Auger point analyses. In this part of the study, scanning electron microscopy (SEM) and scanning Auger microscopy (SAM) were applied to 2024-Al samples which had been immersed for either 5 s or 30 s in the chromate coating bath. In accordance with previous work, the major intermetallic particles observed on the sample surfaces were the irregular-shaped Al-Cu-Fe-Mn and the rounder Al-Cu-Mg second-phase particles [7,10,11,15,16], and our analyses focused on the CCC film growth on such particles and on the alloy matrix in their vicinity. The behavior and appearance of the Al-Cu-Fe-Mn particles was consistent with previous descriptions in the literature [6,9]: namely,

these particles looked intact (sometimes with electrochemically formed peripheral trenches) after the 5 s immersion, and were more definitely covered with CCC after 30 s.

As for the Al-Cu-Mg particles, some of them also looked intact after the 5 s and 30 s immersions, and their behaviors were similar to the Al-Cu-Fe-Mn particles. Fig. 1a shows an example of such an intact Al-Cu-Mg particle, where the white markers show locations used for SAM point analyses. Fig. 1b shows a contrasting Al-Cu-Mg particle, which demonstrates anodic activity and dealloying after the 5 s chromate treatment, as reported earlier [6,10,11]. For this particle, a rough spongy structure developed, and the SAM point analyses confirmed depletion of Mg and Al leaving a surface basically composed of Cu and O. Interestingly, the amounts of Al and Cr vary across the surface, the latter being lower than over the intact particles. It is believed that the particles in Figs. 1a,b start with comparable overall compositions; however, their surfaces become quite different after a 5 s immersion in the chromate bath, and in particular the particle in Fig. 1a still demonstrates a Mg peak in its Auger electron spectra. These different behaviors presumably originate with some initial chemical inhomogeneities [17,18], although this is still to be probed in detail.

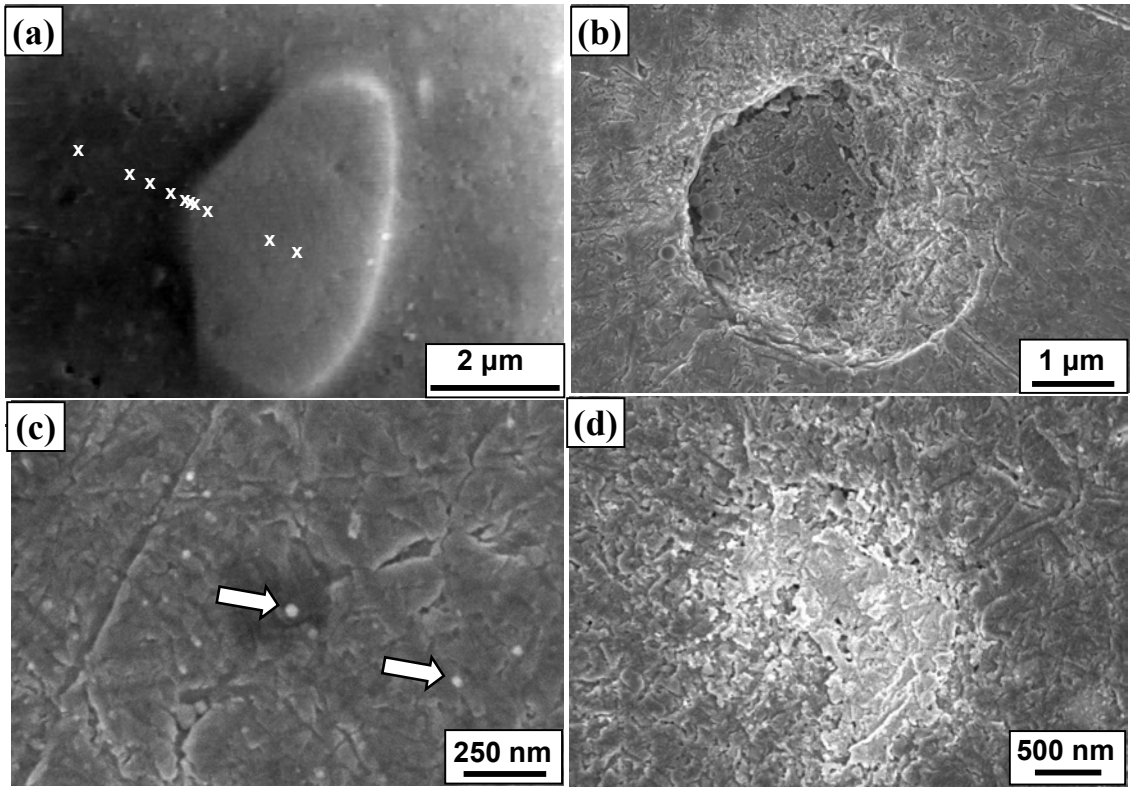

Fig. 1. SEM images from different microstructural regions after chromate treatment for 5 s: (a) Al-Cu-Mg 'intact' particle where crosses show locations of Auger point analysis; (b) dealloyed Al-Cu-Mg particle; (c) alloy matrix with 'nodules' marked by arrows; and for 30 s: (d) dealloyed Al-Cu-Mg particle with rougher surface.

The results of quantitative Auger analyses at different positions across the matrix-particle interface for the intact Al-Cu-Mg particle are presented in Fig. 2a. The Cr/Al ratio is reported to avoid artefacts associated with the varying carbon-based contamination which is inevitably present on the surfaces. Results in Fig. 2a (closed circles) show that after the 5 s chromate treatment, the Cr/Al ratio distribution is relatively constant on the Al-Cu-Mg particles which show no visible dealloying. The ratio is much larger than the values for the adjacent Al matrix, where the amount of Cr is very low and the amount of Al relatively increased compared with the particles. After the 5

s treatment, all Al-Cu-Fe-Mn particles demonstrated comparable trends in Cr/Al ratios to those shown in Fig. 2a (solid circles) for the intact Al-Cu-Mg particles.

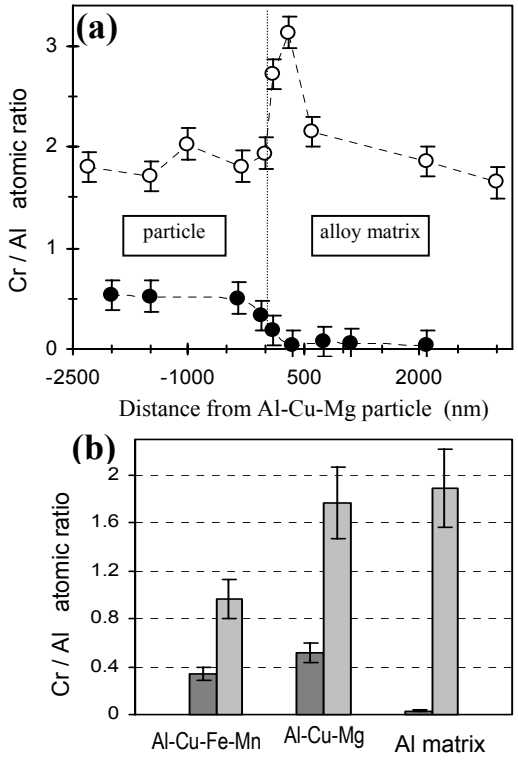

Fig. 2. Cr/Al atomic ratios from SAM for: (a) different positions shown by crosses in Fig. 1(a) after coating for 5s (closed circles) and 30s (open circles); (b) intact Al-Cu-Fe-Mn and Al-Cu-Mg particles, and alloy matrix, after coating for 5 s (dark gray) and 30 s (light gray).

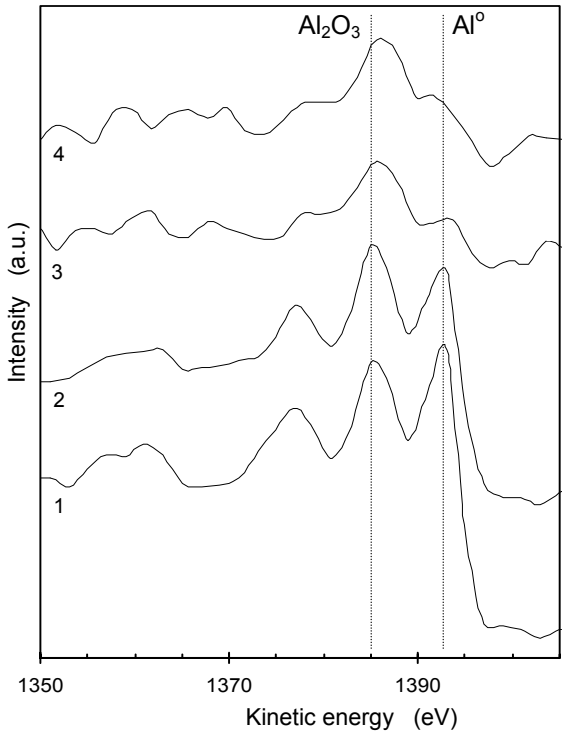

Fig. 3. Al KLL Auger spectra taken from various areas of the sample after coating for 5s: (1) alloy matrix; (2) 'nodule'; and after coating for 30 s: (3) alloy matrix; and (4) 'intact' Al-Cu-Mg particle. The vertical lines identify structure characteristic of metallic and oxide components.

A SEM micrograph to indicate the topography of the alloy matrix after the 5 s immersion is shown in Fig. 1c. In addition to scratches originating with polishing, the effects of acid etching are seen, as well as the appearance of "nodule-like" features (bright round spots up to 50 nm in diameter). In earlier work, these nodules have been supposed to originate with CCC precipitates [6], but Auger electron spectra in the point analysis mode offer the opportunity to assess local composition. The Auger spectra from the nodules turn out to be very similar to those from the alloy matrix, and both appear to be composed mainly of oxidized Al (compare Al KLL spectra numbered (1) and (2) in Fig. 3). No Cr was detected on the nodules, an observation which differs from the view expressed by Brown and Kobayashi that the nodules represent incipient CCC formation on the alloy matrix [6].

In previous discussions of early CCC growth, much attention has been paid to the halos surrounding the electrochemically active particles at the initial stage of film nucleation [6,9]. Such halos, similar to that in Fig. 1b, have been thought to result from local CCC deposition, however the SAM point analysis does not support that view either. A comparable amount of Cr was detected on both the halo-like structure and the alloy matrix, and both were less than over intact second-phase particles for after the 5 s immersion.

Based on observations with SEM and SAM for after the 5 s immersion, the 2024-Al surface has received a discrete coating, with most CCC being located on top of those second-phase particles that appear intact. This finding supplements previous reports by Brown and Kobayashi [6] and by Campestrini *et al.* [9] who also concluded, on the basis of observations with atomic force microscopy and energy dispersive X-ray analysis, that the film initiation occurs over the intermetallic particles. It should also be noted that, although much more CCC was detected over intact particles than over the alloy matrix, surfaces of the intact particles appeared much smoother than the alloy matrix. Apparently fast CCC deposition over the second-phase particles during the first stage of film growth gives a denser and relatively smooth coating [9].

After the 30 s immersion, the 2024-Al surface looks generally rougher, although the coating morphology varies with the underlying microstructure. Fig. 1d gives an example of a previously dealloyed Al-Cu-Mg particle, with its halo-like structure, which is now covered with CCC. The rapid CCC growth over dissolved particles between 5 and 30 s of chromate immersion probably results from the surface becoming porous by the dealloying and by the more cathodic nature of the remnant Al-Cu-Mg particle after dealloying.

SEM micrographs of the matrix after 30 s coating (not shown) demonstrate that a smaller number of "nodules" remain after the longer immersion time. The more pronounced roughness of the matrix surface apparently results from both the extra acid etching and more deposition of amorphous Cr oxide. SAM point analyses at various surface features of the sample, after the 30 s immersion, demonstrate the presence of Cr at all locations, with the amount of Cr being relatively uniform. This implies that the CCC covers the sample surface after 30 s. More detailed analysis of Auger Al KLL spectra revealed appreciable structure characteristic of Al oxide at all surface locations (compare spectra numbered (3) and (4) in Fig. 3). It appears most likely that the Al-oxide components after 30 s originate more from the coating-substrate interfacial regions, a conclusion that supports an assumption of Brown and Kobayashi [6] that the oxide is not completely etched away before the deposition, and that electron transfer occurs through a thin layer of oxidized Al.

Fig. 2a (open circles) reports the distribution of measured Cr/Al ratios over the intact Al-Cu-Mg second-phase particle and the adjacent alloy matrix after 30 s immersion in the CCC bath. The Al-Cu-Fe-Mn particles demonstrate a very similar distribution for the Cr/Al ratio. After 30 s, the sample is fully coated and more uniform, although the CCC thickness is not constant. The interfaces between the underlying second-phase particles and the alloy matrix are still detected insofar as the Cr/Al ratios demonstrate discrete change at their location. Fig. 2b reports average values of the Cr/Al ratio measured over central parts of the intact Al-Cu-Fe-Mn and Al-Cu-Mg particles, and the alloy matrix, for both 5 s and 30 s immersion in the chromate bath. Since the Cr deposition after 5 s is essentially on the particles, it is clear that fast CCC growth occurs over the Al matrix during the 5 s to 30 s period of coating. Also, after the 30 s immersion, the dealloyed second-phase particles are coated with a CCC layer similar to the intact particles.

XPS observations. The composition of CCCs is believed to vary with depth as well as laterally through coatings on 2024-Al alloy [7], although knowledge about how chromate ions accumulate in the growing CCCs remains limited. The amount of Cr(VI) in a coating has been used as an indicator of the ability of a CCC to protect a substrate after a coating has suffered mechanical damage [19,20]. Therefore, the specification of Cr species in coatings has interest, since those with low Cr(VI) content may be expected to be less capable of demonstrating the "self-healing" effect [19-21].

Fig. 4a presents Cr 2p spectra for samples that had been chromate treated for periods ranging from 3 to 120 s. Other samples measured for 5 and 60 s immersions (not shown) also follow the trend shown. It is clear that as a continuous film covers the alloy surface and its thickness increases, the peak at ~577.5 eV binding energy increases and the shoulder at ~580 eV becomes more prominent; the latter component is believed to represent Cr(VI) species incorporating into the

coating. Curve fitting for the Cr $2p_{3/2}$ structure was performed based using three components, assigned as Cr(VI) 579.7 eV, $Cr(OH)_3$ 578.1 eV and Cr_2O_3 576.9 eV, in accordance with Maeda and Yamamoto [22]. Fig. 4b gives an example of such a curve fitting for the sample which had been chromate treated for 1 min. Values of the ratio Cr(VI)/(Cr(III)+Cr(VI)), where Cr(III) includes both oxide and hydroxide components, were measured to equal 0.05, 0.11, 0.13, 0.28, 0.30 and 0.36 for samples treated for 3, 5, 10, 30, 60 and 120 s, respectively. This evidence strongly supports the percentage of Cr(VI) in the coating increasing with the immersion time; further by 2 min this value appears at around 35%.

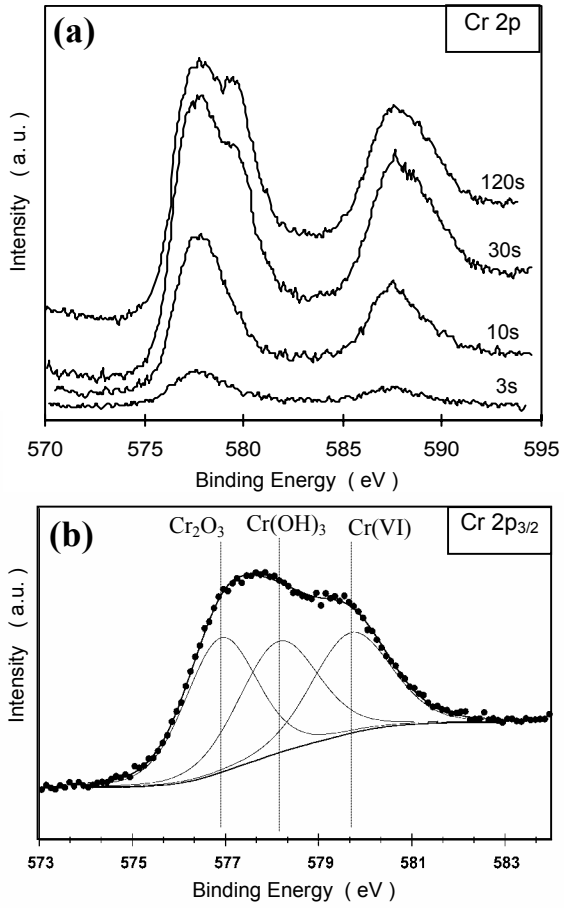

Fig. 4. Cr 2p spectra: (a) after coating for different times; (b) curve fitting for Cr $2p_{3/2}$ after 1 min coating.

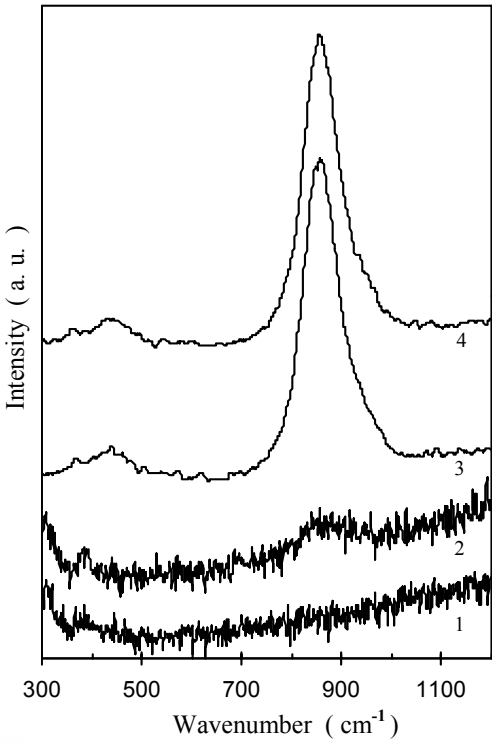

Fig. 5. Raman spectra from Al-Cu-Fe-Mn particle (1,3) and alloy matrix (2,4) after coating for 30 s (1,2) and 2 min (3,4).

The XPS results for incorporation of chromate species into a growing coating show consistency with the SEM and SAM observations. Indeed, as film growth begins first over intermetallic particles, where denser films are expected to form [9], lower incorporation of chromate anions occurs into the discrete and denser Cr(III) hydroxide coatings at this stage. As seen in Fig. 4a, the contribution of Cr(VI) is lower for films prepared for 3-10 s, and SAM showed only traces of Cr can be detected over the alloy matrix for the sample immersed for 5 s. After 30 s, SEM shows that the matrix is rougher, and Auger electron spectroscopy confirms that this is a thicker film with a substantial Cr content. More chromate incorporates into such a film after 30 s, suggesting a possible relationship between Cr(VI) incorporation and surface roughness, although the amounts incorporated change only slightly between the samples immersed for 1 and 2 min. The roughness presumably reflects varying thickness of coating. That factor may be the more important one

according to an argument which starts with the trend in Fig. 4a, where the Cr(VI) to Cr(III) reduction depends on the availability of metallic Al. As the coating grows thicker, this reduction becomes inhibited by the reduced ability of Cr(VI) species to diffuse to the vicinity of cathodic sites at the substrate. After immersion for a few minutes, it appears that the CCC growth becomes suppressed with Cr(VI) ions remaining entrapped within the thicker coating.

For the early stages of coating, an appreciable area of the alloy substrate is exposed directly to the acidic coating solution, resulting in Al oxidation and the associated reduction of Cr(VI) to Cr(III). Then, the amount of Cr(VI) at the alloy-solution interface can be limited by diffusion from the bulk of the solution, and little Cr(VI) gets incorporated unreduced into the coating. During the later stages, the Al dissolution slows and there is less Cr(VI) to Cr(III) reduction, so enabling the supply of Cr(VI) to be maintained to the solution interface. That allows the Cr(VI) adsorption and its subsequent incorporation into the coating.

Raman spectroscopy observations. Fig. 5 shows Raman spectra collected over bigger Al-Cu-Fe-Mn particles and the alloy matrix in samples which had been chromate treated for 30 s and 2 min. This discussion centers on the band at ~860 cm^{-1}, which Xia *et al.* [21] attributed to Cr(III)-O-Cr(VI) formed by a direct bonding interaction between chromate and Cr(III) hydrated oxide. After 30 s, it is apparent that this particular Raman band is not detected over the Al-Cu-Fe-Mn particles, while it is over the alloy matrix. Even though SAM indicated a relatively uniform film thickness across the whole surface after a 30 s immersion, the Raman spectra (1) and (2) imply that Cr(VI) is incorporated non-uniformly into the chromate coating. In contrast to this situation, after the 2 min immersion Raman spectroscopy (see spectra (3) and (4) in Fig. 5) demonstrates the presence of well-pronounced bands at ~860 cm^{-1} over both the alloy matrix and the Al-Cu-Fe-Mn particles. Thus, while the Cr(VI) incorporation is non-uniform at the earliest stages of CCC growth on the 2024-Al surface, later a more uniform distribution of Cr(VI) occurs, as the film thickness and roughness increase (e.g. after immersion for 1 min or more).

The Raman results reinforce those from XPS in that both indicate a tendency for Cr(VI) species to accumulate first in the rougher CCC film over the alloy matrix rather than over the second-phase particles, where the films are expected to be denser [9]. As the coating continues to grow, it becomes rougher over the whole surface, which leads to the gradual incorporation of chromate anions over the particles as well. Our observations with Raman spectroscopy of Cr(VI) species over intermetallic particles differ from the report of McGovern *et al.* [16], who used the same technique but concluded the opposite when a 2024-Al sample was treated in an Alodine chromating bath for 5 min. The difference likely relates to the different natures of the chromating baths used, and in particular the fact that our bath did not include ferricyanide. That is a component of the commercial bath and is believed to inhibit CCC growth over Cu-containing particles [16]. Also it is noted that Kolics *et al*. [11] did observe significantly thicker CCC over the intermetallic particles, than over the alloy matrix, when ferricyanide was not present in a corrosive solution with chromate inhibitor.

Conclusions.

A combination of surface science techniques used has been demonstrated to be effective for probing the initial and further growth of chromate conversion coatings on 2024-Al alloy. The process was confirmed to depend closely on the microstructure of the alloy, consistently with other work [6,7,9,16]. By using scanning Auger microscopy, a spatially-resolved chemical analysis technique, the coating growth is shown to initiate at those second-phase intermetallic particles which act cathodically, and subsequently on the surface of the alloy matrix. After immersion in the coating bath for 5 s, the chromate coating is detected over the second-phase particles that look intact, whereas only traces of Cr could be found over the Al matrix. No support was found for the interpretation that the surface “nodules”, formations on the alloy matrix of up to 50 nm in diameter,

are incipient deposits of a Cr(III) oxide; rather it appears that these features are basically oxidized aluminum.

While the initial growth found on Al-Cu-Fe-Mn intermetallics is in good agreement with the model of Campestrini *et al.* [9], it is more complex over the Al-Cu-Mg particles insofar as some of them experience severe dealloying during the first few seconds of chromate treatment. Those Al-Cu-Mg particles which appear intact follow a growth mechanism like that on the Al-Cu-Fe-Mn intermetallics, and act as cathodic sites for the Cr(VI) to Cr(III) reduction. It is proposed that the different behaviors among the Al-Cu-Mg second-phase particles result from differences in their local chemical composition, which may be affected to some degree by the sample pretreatment (polishing).

On the Al matrix, coating growth occurs between 5-30 s of immersion, being faster at this stage than over the intermetallic particles. After 30 s chromating, the alloy surface is completely covered with a relatively uniform thickness. The coating-alloy interface contains oxidized Al at all locations investigated, including both the alloy matrix and the second-phase particles.

XPS and Raman analyses demonstrate that Cr(VI) incorporation into a coating occurs mainly at the later stages of film growth, apparently resulting from the more-developed surface roughness which develops in the coatings after the longer immersion times. Chromate accumulates both at the intermetallic sites and over the alloy matrix when the chromating solution contains no ferricyanide additive.

Acknowledgements

We are grateful for the support provided for this research by the Natural Sciences and Engineering Research Council of Canada, and thank Prof. D. Bizzotto and Dr. L. Zhu for the Raman measurements.

References

[1] J.E. Gray and B. Luan: J. Alloy. Compd. Vol.336 (2002), p.88.

[2] W.J. van Ooij, D.Q. Zhu, G. Prasad, S. Jayaseelan, Y. Fu and N. Teredesai: Surf. Eng. Vol.16 (2000), p.386.

[3] H. Guan and R.G. Buchheit: Corrosion Vol.60 (2004), p.284.

[4] Y. Liu, D. Sun, H. You and J.S. Chung: Appl. Surf. Sci. Vol.246 (2005), p.82.

[5] A.S. Akhtar, D. Susac, P. Glaze, K.C. Wong, P.C. Wong and K.A.R. Mitchell: Surf. Coat. Technol. Vol.187 (2004), p.208.

[6] G.M. Brown and K. Kobayashi: J. Electrochem. Soc. Vol.148 (2001), p.B457.

[7] M. Jaime Vasquez, G.P. Halada, C.R. Clayton and J.P. Longtin: Surf. Interface Anal. Vol.33 (2002), p.607.

[8] D. Susac, X. Sun, R.Y. Li, K.C. Wong, P.C. Wong, K.A.R. Mitchell and R. Champaneria: Appl. Surf. Sci. Vol.239 (2004), p.45.

[9] P. Campestrini, H. Terryn, J. Vereecken and J.H.W. de Wit: J. Electrochem. Soc. Vol.151 (2004), p.B359.

[10] R.G. Buchheit, R.P. Grant, P.F. Hlava, B. Mckenzie and G.L. Zender: J. Electrochem. Soc. Vol.144 (1997), p.2621.

[11] A. Kolics, A.S. Besing and A. Wieckowski: J. Electrochem. Soc. Vol.148 (2001), p.B322.

[12] J.R. Waldrop and M.W. Kendig: J. Electrochem. Soc. Vol.145 (1998), p.L11.

[13] X. Sun, R. Li, K.C. Wong and K.A.R. Mitchell: J. Mater. Sci. Vol.36 (2001), p.3215.

[14] A.S. Akhtar, D. Susac, K.C. Wong, P.C. Wong and K.A.R. Mitchell: Mater. Sci. Forum, submitted for this volume.

[15] A.E. Hughes, R.J. Taylor and B.R.W. Hinton: Surf. Interface Anal. Vol.25 (1997), p.223.

[16] W.R. McGovern, P. Schmutz, R.G. Buchheit and R.L. McCreery: J. Electrochem. Soc. Vol.147 (2000), p.4494.

[17] G.S. Frankel: J. Electrochem. Soc. Vol.145 (1998), p.2186.

[18] P. Schmutz and G.S. Frankel: J. Electrochem. Soc. Vol.145 (1998), p.2295.

[19] F.W. Lytle, R.B. Greegor, G.L. Bibbins, K.Y. Blohowiak, R.E. Smith and G.D. Tuss: Corros. Sci. Vol.37 (1995), p.349.

[20] J. Zhao, L. Xia, A. Sehgal, D. Lu, R.L. McCreery and G.S. Frankel: Surf. Coat. Technol. Vol.140 (2001), p.51.

[21] L. Xia and R.L. McCreery: J. Electrochem. Soc. Vol.145 (1998), p.3083.

[22] S. Maeda and M. Yamamoto: Prog. Org. Coat. Vol.33 (1998), p.83.

Aluminium Alloys 2006 - ICAA10
10.4028/www.scientific.net/MSF.519-521

Surface Science Studies of the Effect of Al Alloy Microstructure on the Formation of Chromate Coatings
10.4028/www.scientific.net/MSF.519-521.621

DOI References
[2] W.J. van Ooij, D.Q. Zhu, G. Prasad, S. Jayaseelan, Y. Fu and N. Teredesai: Surf. Eng. Vol.16 (2000), .386.
doi:10.1179/026708400101517369
[3] H. Guan and R.G. Buchheit: Corrosion Vol.60 (2004), p.284.
doi:10.5006/1.3287733
[6] G.M. Brown and K. Kobayashi: J. Electrochem. Soc. Vol.148 (2001), p.B457.
doi:10.1149/1.1409544
[7] M. Jaime Vasquez, G.P. Halada, C.R. Clayton and J.P. Longtin: Surf. Interface Anal. Vol.33 (2002), .607.
doi:10.1002/sia.1428
[8] D. Susac, X. Sun, R.Y. Li, K.C. Wong, P.C. Wong, K.A.R. Mitchell and R. Champaneria: Appl. Surf. ci. Vol.239 (2004), p.45.
doi:10.1016/S0169-4332(04)00591-4
[9] P. Campestrini, H. Terryn, J. Vereecken and J.H.W. de Wit: J. Electrochem. Soc. Vol.151 (2004), .B359.
doi:10.1149/1.1736682
[11] A. Kolics, A.S. Besing and A. Wieckowski: J. Electrochem. Soc. Vol.148 (2001), p.B322.
doi:10.1149/1.1380674
[12] J.R. Waldrop and M.W. Kendig: J. Electrochem. Soc. Vol.145 (1998), p.L11.
doi:10.1149/1.1838199
[13] X. Sun, R. Li, K.C. Wong and K.A.R. Mitchell: J. Mater. Sci. Vol.36 (2001), p.3215.
doi:10.1023/A:1017986319654
[16] W.R. McGovern, P. Schmutz, R.G. Buchheit and R.L. McCreery: J. Electrochem. Soc. Vol.147 2000), p.4494.
doi:10.1149/1.1394091
[17] G.S. Frankel: J. Electrochem. Soc. Vol.145 (1998), p.2186.
doi:10.1149/1.1838748
[18] P. Schmutz and G.S. Frankel: J. Electrochem. Soc. Vol.145 (1998), p.2295.
doi:10.1149/1.1838748
[22] S. Maeda and M. Yamamoto: Prog. Org. Coat. Vol.33 (1998), p.83.
doi:10.1080/09670269810001736563
[2] W.J. van Ooij, D.Q. Zhu, G. Prasad, S. Jayaseelan, Y. Fu and N. Teredesai: Surf. Eng. Vol.16 (2000), p.386.
doi:10.1179/026708400101517369
[7] M. Jaime Vasquez, G.P. Halada, C.R. Clayton and J.P. Longtin: Surf. Interface Anal. Vol.33 (2002), p.607.
doi:10.1002/sia.1428
[8] D. Susac, X. Sun, R.Y. Li, K.C. Wong, P.C. Wong, K.A.R. Mitchell and R. Champaneria: Appl. Surf. Sci. Vol.239 (2004), p.45.

doi:10.1016/S0169-4332(04)00591-4
[9] P. Campestrini, H. Terryn, J. Vereecken and J.H.W. de Wit: J. Electrochem. Soc. Vol.151 (2004), p.B359.
doi:10.1149/1.1736682
[16] W.R. McGovern, P. Schmutz, R.G. Buchheit and R.L. McCreery: J. Electrochem. Soc. Vol.147 (2000), p.4494.
doi:10.1149/1.1394091